

Stability Analysis on Stagnation-Point Flow and Heat Transfer towards a Permeable Stretching/Shrinking Sheet with Heat Source in a Casson Fluid


 Open
Access

 Ubaidullah Yashkun^{1,2}, Fatinnabila Kamal¹, Khairy Zaimi^{1,*}, Nor Ashikin Abu Bakar¹, Norshaza Atika Saidin¹
¹ Institute of Engineering Mathematics, Universiti Malaysia Perlis, Pauh Putra Campus, 02600 Arau, Perlis, Malaysia

² Sukkur IBA University, Airport Road, Sukkur, 65200, Sindh, Pakistan

ARTICLE INFO

Article history:

Received 19 April 2020

Received in revised form 17 June 2020

Accepted 23 June 2020

Available online 29 June 2020

ABSTRACT

This paper deals with a stagnation-point boundary layer flow and heat transfer of a Casson fluid towards a stretching/shrinking sheet. The main objective of the present study is to analyse the effects of the injection parameter and heat source on the velocity and temperature profiles as well as the skin friction coefficient and the Nusselt number. It is vital to study the heat transfer and fluid flow problems in the presence of injection and heat source effects due to a wide variety of applications in engineering and industry. The governing nonlinear partial differential equations are transformed into a system of nonlinear ordinary differential equations by using similarity transformation, before being solved numerically using the boundary value problem solver *bvp4c* routine in MATLAB. Dual solutions are found to exist for the shrinking sheet case, whereas the solution is unique for the stretching case. The stability analysis has been performed to determine the stable solution. It is shown that the first solutions are stable and physically reliable while the second solutions are not. Further, the present results have been compared with the previous published results for a particular case and the comparisons are found to be in good agreement. The local Nusselt number is decreases with an increase in heat source parameter. Rising values of the injection parameter has decreases both the skin friction coefficient and the local Nusselt number.

Keywords:

stability analysis; stagnation point flow;

heat transfer; heat source; injection

effect; Casson fluid

Copyright © 2020 PENERBIT AKADEMIA BARU - All rights reserved

1. Introduction

Stagnation-point is a rest point in the moving fluid. The stagnation-point region encounters the highest pressure, the highest heat transfer and the highest rates of mass decomposition, exists on all solid bodies moving in a fluid (Patel and Timol [1]). Hiemenz was the first who examined the two-dimensional flow of a fluid near a stagnation-point. He was demonstrated that the governing flow

* Corresponding author.

E-mail address: khairy@unimap.edu.my (Khairy Zaimi)

<https://doi.org/10.37934/cfdl.12.6.115>

equations of Navier-Stokes equations can be reduced to an ordinary differential equation of third order using similarity transformation. Stagnation-point flow is continuing to be an interesting area of research among scientists and investigators due to its importance in a wide variety applications both in industrial and engineering processes such as cooling of electronic devices by fans, cooling of nuclear reactors during emergency shutdown, polymer extrusion, wire drawing and drawing of plastic sheets (Makinde *et al.*, [2]). Since then, many investigators have extended the idea to different aspect of the stagnation-point flow problems. Nandy and Pop [3] studied the effects of magnetic field and thermal radiation on the stagnation flow and heat transfer of a nanofluid over a shrinking surface. Later, Fauzi *et al.*, [4] investigated the effect of the slip parameter on the stagnation-point flow and heat transfer over a nonlinear shrinking sheet. Besides that, the problem of the stagnation-point flow of Maxwell fluid towards a permeable surface in the presence of nanoparticles has been considered by Ramesh *et al.*, [5]. Furthermore, Mahapatra and Gupta [6] studied the steady two-dimensional stagnation-point flow of an incompressible viscous fluid over a flat deformable sheet when the flow is started impulsively from rest and suddenly stretched in its own plane with a velocity proportional to the distance from the stagnation-point. Nazar *et al.*, [7] presented the unsteady two-dimensional stagnation-point flow of an incompressible viscous fluid over a flat deformable sheet when the flow is started impulsively from rest and suddenly stretched in its own plane with a velocity proportional to the distance from the stagnation-point. More studies on the stagnation-point flow include those by Othman *et al.*, [8], Rehman *et al.*, [9], Naganthran *et al.*, [10] and Sharma *et al.*, [11].

Problems involving fluid flow over stretching or shrinking surfaces can be found in many industrial manufacturing processes such as hot rolling, paper production, metal spinning, drawing plastic films, glass blowing, continuous casting of metals and spinning of fibers (Roşca and Pop [12]). Due to the numerous applications, the study of stretching/shrinking sheet was subsequently extended by many authors to explore various aspects of skin friction coefficient and heat transfer in a fluid. For example, Yasin *et al.*, [13] numerically examined the steady two-dimensional magnetohydrodynamic flow past a permeable stretching/shrinking sheet with radiation effects. Recently, Naganthran *et al.*, [14] investigated the unsteady stagnation-point flow and heat transfer of a special third grade fluid past a permeable stretching/shrinking sheet. Since then, many researchers have been working on the stretching or shrinking sheet with various physical conditions such as Alam *et al.*, [15], Jamaludin *et al.*, [16], Jusoh *et al.*, [17], Nasir *et al.*, [18], Seth *et al.*, [19], Hamid *et al.*, [20], Soid *et al.*, [21], Dero *et al.*, [22] and Yashkun *et al.*, [23].

Casson fluid is defined as a shear thinning liquid which is assumed to have an infinite viscosity when rate of shear is zero, a yield stress below which no flow occurs and a zero viscosity at an infinite rate of shear (Dash *et al.*, [24]). Casson fluid is one of the non-Newtonian fluids, which has attracted much attention because of their extensive variety of applications in engineering and industry especially in extraction of crude oil from petroleum products, production of plastic materials and syrup drugs (Animasaun *et al.*, [25]). Hayat *et al.*, [26] investigated the mixed convection stagnation-point flow of a Casson fluid with convective boundary conditions. On the other hand, Bhattacharyya [27] analyzed the steady boundary layer stagnation-point flow of a Casson fluid and heat transfer towards a stretching/shrinking sheet. This work has been extended by Kameswaran *et al.*, [28] with the inclusion of Soret and Dufour effects over a stretching sheet. Afterwards, the researcher explored the behaviour of the Casson fluid under various effect and circumstances (see El-Aziz and Yahya [29], Abdul Hakeem *et al.*, [30], Khan *et al.*, [31], Maity *et al.*, [32], Medikare *et al.*, [33], Raju and Sandeep [34-35], Raju *et al.*, [36], Rehman *et al.*, [37], Shateyi *et al.*, [38], and Alkasasbeh [39]).

In this paper, we analyze the behavior of the stagnation-point flow and heat transfer towards a stretching/shrinking sheet with heat source and injection effects in a Casson fluid. This study is an extension of the previous work done by Bhattacharyya [27]. Different from that investigated by

Bhattacharyya [27], we consider the injection effect and heat source effects into flow. The effects of injection and heat source on the velocity profile, temperature profile, skin friction coefficient and local Nusselt number will be presented and discussed. The dual solutions are expected to exist for the shrinking case. A temporal stability analysis is conducted to verify which solution is stable and has real physical implication. Practically, the investigations of the stagnation-point flow and heat transfer over a permeable stretching/shrinking sheet with the inclusion of injection and heat source effects is very significant and beneficial particularly in many industrial manufacturing processes. Even though many investigations on the stagnation-point fluid flow problems have been examined, there are still limited published results and articles found on the injection and heat source impacts. We believe that the present results are new, original and have not been published elsewhere.

2. Methodology

Consider the steady two-dimensional stagnation-point flow of an incompressible Casson fluid located at $y=0$, with the flow being confined in $y>0$. It is assumed that the velocity of the stretching/shrinking sheet is $u_w(x) = ax$, where $a > 0$ is for the stretching sheet and $a < 0$ is for the shrinking sheet, while the free stream velocity is $U_e(x) = bx$ where b is a positive constant. We also assume that the surface temperature T_w is constant. The physical model and the coordinate system is shown in Figure 1, where the x -axis is taken along the direction of the stretching/shrinking sheet and the y -axis is measured normal to it. The rheological equations of the state for an isotropic and incompressible flow of the Casson fluid is given by (see Bhattacharyya [27,40])

$$\tau_{ij} = \begin{cases} 2(\mu_B + p_y / \sqrt{2\pi}) e_{ij}, & \pi > \pi_c, \\ 2(\mu_B + p_y / \sqrt{2\pi_c}) e_{ij}, & \pi < \pi_c, \end{cases} \quad (1)$$

where μ_B is plastic dynamic viscosity of the non-Newtonian fluid, p_y is the yield stress of fluid, π is the product of the component of deformation rate with itself, namely $\pi = e_{ij}e_{ij}$, e_{ij} is the (i, j) -th component of deformation rate and π_c is a critical value of π based on non-Newtonian model.

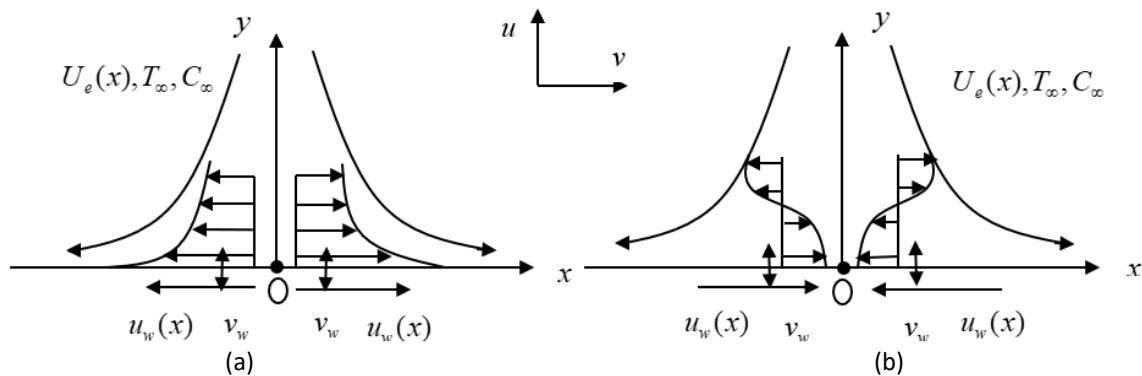


Fig. 1. Physical model and coordinate system: (a) Stretching sheet, (b) Shrinking sheet

Under above conditions, the boundary layer equations can be written as:

$$\frac{\partial u}{\partial x} + \frac{\partial v}{\partial y} = 0, \quad (2)$$

$$u \frac{\partial u}{\partial x} + v \frac{\partial u}{\partial y} = u_e \frac{du_e}{dx} + \nu \left(1 + \frac{1}{\beta} \right) \frac{\partial^2 u}{\partial y^2}, \quad (3)$$

$$u \frac{\partial T}{\partial x} + v \frac{\partial T}{\partial y} = \frac{\kappa}{\rho C_p} \frac{\partial^2 T}{\partial y^2} + \frac{Q_0}{\rho C_p} (T - T_\infty), \quad (4)$$

where u and v are the velocity components in the x and x directions, respectively, ν is the kinematic viscosity, $\beta = \mu_B \sqrt{2\pi_c} / p_y$ is the Casson fluid parameter, κ is the thermal diffusivity, ρ is the density, C_p is the specific heat and Q_0 is the temperature dependent heat generation/absorption.

We assume that Eqs. (2)-(4) are subjected to the boundary conditions:

$$\begin{aligned} u(x, 0) = u_w(x), \quad v(x, 0) = v_0, \quad T(x, 0) = T_w, \\ u(x, y) \rightarrow U_e(x), \quad T(x, y) \rightarrow T_\infty, \quad \text{as } y \rightarrow \infty. \end{aligned} \quad (5)$$

We look for a similarity solution of Eqs. (2) - (4) of the following form:

$$\psi = (\nu x U_e)^{\frac{1}{2}} f(\eta), \quad \theta(\eta) = \frac{T - T_\infty}{T_w - T_\infty}, \quad \eta = \left(\frac{U_e}{\nu x} \right)^{\frac{1}{2}} y, \quad (6)$$

where $\psi(x, y)$ is the stream function defined as $u = \frac{\partial \psi}{\partial y}$ and $v = -\frac{\partial \psi}{\partial x}$, which identically satisfies Eq. (2). By substituting Eq. (6) into Eqs. (3) and (4), the following ordinary differential equations are obtained:

$$\left(1 + \frac{1}{\beta} \right) f''' + ff'' - f'^2 + 1 = 0, \quad (7)$$

$$\theta'' + \text{Pr}(f\theta' + Q\theta) = 0. \quad (8)$$

The boundary conditions in Eq. (5) become

$$\begin{aligned} f(0) = \gamma, \quad f'(0) = \varepsilon, \quad \theta(0) = 1, \\ f'(\eta) \rightarrow 1, \quad \theta(\eta) \rightarrow 0 \quad \text{as } \eta \rightarrow \infty. \end{aligned} \quad (9)$$

Here, $Pr = \frac{\mu C_p}{\kappa}$ is the Prandtl number, $Q = \frac{Q_0}{\rho C_p b}$ is the heat source parameter, $\gamma = -\frac{v_0}{\sqrt{bv}} < 0$ is the injection parameter, $\varepsilon = a/b$ is the stretching ($\varepsilon > 0$) or shrinking ($\varepsilon < 0$) parameter and prime denotes differentiation with respect to η .

The physical quantities of interest are the skin friction coefficient, C_f and the local Nusselt number, Nu_x which are defined as

$$C_f = \frac{\tau_w}{\rho u_e^2(x)}, \quad Nu_x = \frac{xq_w}{k(T_w - T_\infty)}. \quad (10)$$

Here, τ_w is the skin friction or surface shear stress along the plate and q_w is the heat flux from the plate which are given by

$$\tau_w = \mu \left(\frac{\partial u}{\partial y} \right)_{y=0}, \quad q_w = -k \left(\frac{\partial T}{\partial y} \right)_{y=0}, \quad (11)$$

where k is the fluid thermal conductivity.

Substituting Eq. (6) into Eq. (11) and using Eq. (10), the following expression are obtained

$$Re_x^{1/2} C_f = \left(1 + \frac{1}{\beta} \right) f''(0), \quad Re_x^{-1/2} Nu_x = -\theta'(0), \quad (12)$$

where $Re_x = \frac{U_e x}{\nu}$ is the local Reynolds number.

3. Stability Analysis

Following Weidman *et al.*, [41], to study the temporal stability of the solutions of Eqs. (7)-(8) subject to boundary conditions in Eq. (9), we consider the unsteady case for Eqs. (3)-(4) which are replaced by

$$\frac{\partial u}{\partial t} + u \frac{\partial u}{\partial x} + v \frac{\partial u}{\partial y} = U_e \frac{dU_e}{dx} + v \left(1 + \frac{1}{\beta} \right) \frac{\partial^2 u}{\partial y^2}, \quad (13)$$

$$\frac{\partial T}{\partial t} + u \frac{\partial T}{\partial x} + v \frac{\partial T}{\partial y} = \frac{\kappa}{\rho C_p} \frac{\partial^2 T}{\partial y^2} + \frac{Q_0}{\rho C_p} (T - T_\infty), \quad (14)$$

where t denotes the time. The new similarity transformation of the unsteady-state problem by considering dimensionless time variable τ is introduced as

$$\eta = y\sqrt{\frac{b}{\nu}}, u = bx\frac{\partial f}{\partial \eta}(\eta, \tau), v = -\sqrt{b\nu}f(\eta, \tau), \quad (15)$$

$$T = T_\infty + (T_w - T_\infty)\theta(\eta, \tau), \tau = bt.$$

By substituting Eq. (15) into Eqs. (13) and (14), the following equations are obtained:

$$\left(1 + \frac{1}{\beta}\right)\frac{\partial^3 f}{\partial \eta^3} + f\frac{\partial^2 f}{\partial \eta^2} - \left(\frac{\partial f}{\partial \eta}\right)^2 + 1 - \frac{\partial^2 f}{\partial \eta \partial \tau} = 0, \quad (16)$$

$$\frac{1}{Pr}\frac{\partial^2 \theta}{\partial \eta^2} + f\frac{\partial \theta}{\partial \eta} + Q\theta - \frac{\partial \theta}{\partial \tau} = 0, \quad (17)$$

subject to boundary conditions

$$f(0, \tau) = \gamma, \frac{\partial f}{\partial \eta}(0, \tau) = \varepsilon, \theta(0, \tau) = 1,$$

$$\frac{\partial f}{\partial \eta}(\eta, \tau) = 1, \theta(\eta, \tau) = 0, \text{ as } \eta \rightarrow \infty. \quad (18)$$

To test the stability of the steady flow and heat transfer solution, $f(\eta) = f_0(\eta)$ and $\theta(\eta) = \theta_0(\eta)$ satisfying the boundary value problem in Eqs. (7)-(9), let us write (see Weidman *et al.*, [41])

$$f(\eta, \tau) = f_0(\eta) + e^{-\lambda\tau}F(\eta), \quad (19)$$

$$\theta(\eta, \tau) = \theta_0(\eta) + e^{-\lambda\tau}G(\eta),$$

where λ is an unknown eigenvalue, and $F(\eta)$ and $G(\eta)$ are small relative to $f_0(\eta)$ and $\theta_0(\eta)$. Solutions of the eigenvalue problem in Eqs. (16)-(18) give an infinite set of eigenvalues $\lambda_1 < \lambda_2 < \lambda_3 \dots$, if λ_1 is negative, there is an initial growth of disturbances and the flow is unstable but when λ_1 is positive, there is an initial decay and the flow is stable.

By substituting Eq. (19) into Eqs. (16) and (17), one obtains the following linearized problem:

$$\left(1 + \frac{1}{\beta}\right)F''' + f_0F'' + f_0'F - (2f_0' - \lambda)F' = 0, \quad (20)$$

$$\frac{1}{Pr}G'' + f_0G' + F\theta_0' + (Q + \lambda)G = 0, \quad (21)$$

along with the following boundary conditions:

$$\begin{aligned}
 F(0) = 0, F'(0) = 0, G(0) = 0, \\
 F'(\eta) = 0, G(\eta) = 0 \text{ as } \eta \rightarrow \infty.
 \end{aligned}
 \tag{22}$$

It should be mentioned that for particular values of Pr , Q , γ and ε , the stability of the corresponding steady flow solution $f_0(\eta)$ and $\theta_0(\eta)$ is determined by the smallest eigenvalue λ .

4. Results

The ordinary differential Eqs. (7) and (8) subject to the boundary conditions in Eq. (9), were solved numerically using the `bvp4c` function in Matlab software. The results from the numerical solution are presented in terms of the skin friction coefficient $Re_x^{1/2} C_f$, the local Nusselt number (represents the heat transfer rate) $Re_x^{-1/2} Nu_x$ velocity profile, $f'(\eta)$ and temperature profile, $\theta(\eta)$ for different values of the non-dimensional parameters, namely the injection parameter γ , stretching/shrinking parameter ε and heat source parameter Q , while the Prandtl number Pr is fixed at $Pr=1$ for the comparison.

For the validation purpose, we have compared the numerical results with those reported by Mahapatra and Gupta [6], and Bhattacharyya [27]. Table 1 shows the comparison values of $\theta'(0)$ with those of Mahapatra and Gupta [6] for the case of a stretching sheet without injection and heat source effects by setting $\beta \rightarrow \infty$ and $Q=0$ in Eqs. (7) and (8), $f'(0)=1$ and $f(0)=0$ in the boundary conditions in Eq. (9) and $a/c=1$ in Eqs. (12)-(13) of the paper by Mahapatra and Gupta [6]. The present results were also compared with those obtained by Bhattacharyya [27] for the case of Newtonian fluid case ($\beta \rightarrow \infty$), without heat source ($Q=0$) in Eqs. (7) and (8), injection effect is absent, i.e. $f(0)=0$ in the boundary conditions in Eq. (9) and $c/a=1$ in Eq. (10) of the paper by Bhattacharyya [27] for several values of ε as presented in Table 2. Both comparisons are found to be in a very good agreement, and thus we are confident that the present numerical results are correct and accurate.

Table 1

Comparison of the values $\theta'(0)$ with those of Mahapatra and Gupta [6] for the case of a stretching sheet in Newtonian fluid case without injection and heat source effects by setting $\beta \rightarrow \infty$ and $Q=0$ in Eqs. (7) and (8), $f'(0)=1$ and $f(0)=0$ in the boundary conditions in Eq. (9) and taking $a/c=1$ in Eqs. (12)-(13) of the paper by Mahapatra and Gupta [6]

Pr	Mahapatra and Gupta [6]	Present study
0.05	-0.178	-0.178413806
0.1		-0.252313245
0.5	-0.563	-0.564189588
1.0	-0.796	-0.797884572
1.5	-0.974	-0.977205026
2.0		-1.128379165
3.0		-1.381976604
4.0		-1.595769135
5.0		-1.784124125

Figures 2-4 demonstrate the variation of the skin friction coefficient $Re_x^{1/2} C_f$ and the local Nusselt number $Re_x^{-1/2} Nu_x$ with ε for some values of γ and Q when β and Pr are fixed. For these Figures 2-4, the solid lines representing first (upper branch) solution while the dotted lines indicate the second (lower branch) solution. Based on Figures 2-4, the dual solutions exist for a certain range of the shrinking strength. Thus, there is a necessity to conduct the stability analysis to verify which solution could be utilized in the real world phenomena. A stability analysis is carried out by solving eigenvalue problems in Eqs. (20)-(21) with boundary conditions in Eq. (22). The stable solution is identified based on the positive smallest eigenvalues λ , whereas the unstable solution is recognized based on the negative smallest eigenvalues λ . Positive values of λ gives an initial decay of disturbance which results in a stable flow, whereas negative values of λ results in the growth of disturbance and causes an unstable flow. For the present problem, the smallest eigenvalues, λ_1 at several values of ε when $\beta=5$, $\gamma=-0.2$ and $Pr=Q=1$ are tabulated in Table 3, which reports that the smallest eigenvalues are $\lambda_1 > 0$ for the first solution and $\lambda_1 < 0$ for the second solution. So, the first solution is stable and is physically reliable while the second solution is unstable.

Table 2

Comparison of the values $f''(0)$ with those of Bhattacharyya [27] for the case of Newtonian fluid case ($\beta \rightarrow \infty$), without heat source effect ($Q=0$) in Eqs. (7) and (8), neglecting injection effect ($f(0)=0$) in the boundary conditions in Eq. (9) and taking $c/a = \varepsilon$ in Eq. (10) of the paper by Bhattacharyya [27] for both stretching/shrinking sheet

ε	Bhattacharyya [27]	Present study
0	1.2325878	1.232587653
0.1	1.1465608	1.146560998
0.2	1.0511299	1.051129992
0.3		0.946816117
0.4		0.834072086
0.5	0.7132951	0.713294954
0.8		0.306094758
1.0	0	0
-0.25	1.4022405	1.402240807
-0.5	1.4956697	1.495669765
-0.6		1.507024704
-0.7		1.500360770
-0.75	1.4892981	1.489298235
-0.8		1.472388354
-0.9		1.418077379
-1.0	1.3288169 (0)	1.328816865 (0)
-1.05		1.266227907 (0.012177915)
-1.1	1.1866806 (0.0492286)	1.186680255 (0.049228945)
-1.15	1.0822316 (0.1167023)	1.082231137 (0.116702101)
-1.2	0.9324728 (0.2336491)	0.932473321 (0.233649679)
-1.22		0.845110242 (0.308849262)
-1.24	0.7066020 (0.4356712)	0.706605223 (0.435672076)

() second solution

Table 3

Smallest eigenvalue, λ_1 for some values of ε when $\beta = 5$, $\gamma = -0.2$ and $Pr = Q = 1$

ε	First solution (Upper branch), λ_1	Second solution (Lower branch), λ_1
-1.1	0.6984	-
-1.13	0.5215	-
-1.16	0.2521	-0.2388
-1.163	0.2084	-0.1993
-1.166	0.1535	-0.1485
-1.169	0.0633	-0.0625
-1.1693	0.0457	-0.0453
-1.1696	0.0136	-0.0136

Figures 2 and 3 show the variations of the skin friction coefficient and the local Nusselt number, respectively, for different values of injection parameter γ . From Figures 2-3, it is found that it is possible to obtain dual solutions of the similarity equations in Eqs. (7) and (8) subject to the boundary conditions in Eq. (9). These Figures 2-3 indicate that there are dual solutions for $\varepsilon_c \leq \varepsilon < -1$, unique solutions for $\varepsilon \geq -1$ and no solutions obtained for $\varepsilon < \varepsilon_c < 0$, where ε_c is the critical values of ε for which Eqs. (7) and (8) have no solutions and the full Navier–Stokes and energy equations should be solved. Based on our computation, the critical values ε_c obtained for $\gamma = 0, -0.2$ and -0.4 are $\varepsilon_{c1} = -1.24657$, $\varepsilon_{c2} = -1.16962$ and $\varepsilon_{c3} = -1.10580$, respectively as shown in Figures 2- 3.

Figure 2 reveals the skin friction coefficient $Re_x^{1/2} C_f$ appears to decrease with increasing magnitude of injection parameter γ . This is because of injection effect that decreasing the surface shear stress, delay the fluid flow and thus, decrease the velocity gradient at the surface which is consistent with the graph in Figure 5. As it can be seen in Figures 2 and 3, the values of $|\varepsilon_c|$ increase with decreasing of magnitude γ suggests that reducing injection effect increases the range of existence of solutions to the similarity equations in Eqs. (7) and (8) subject to boundary conditions in Eq. (9). Physically, decreasing γ appears to delay the boundary layer separation.

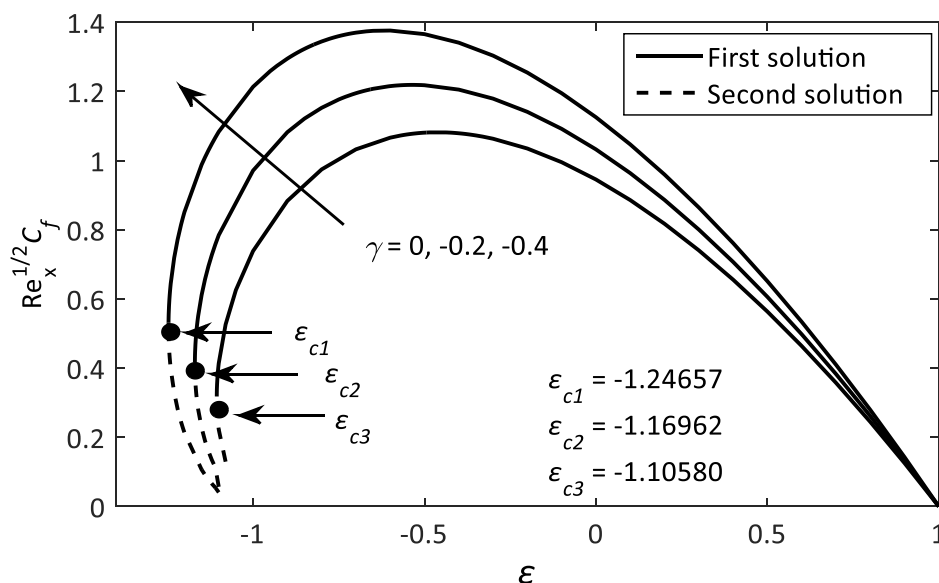


Fig. 2. Variation of the skin friction coefficient $Re_x^{1/2} C_f$ with ε for different values of γ when $Pr = 1, Q = 1$ and $\beta = 5$

Figure 3 displays the variation in the local Nusselt number as a function of the stretching/shrinking parameter ε with some values of the injection parameter γ . As the magnitude of γ increases, the temperature gradient at the surface decreases. As a result, the heat transfer rate at the surface decreases with the increasing magnitude of injection parameter.

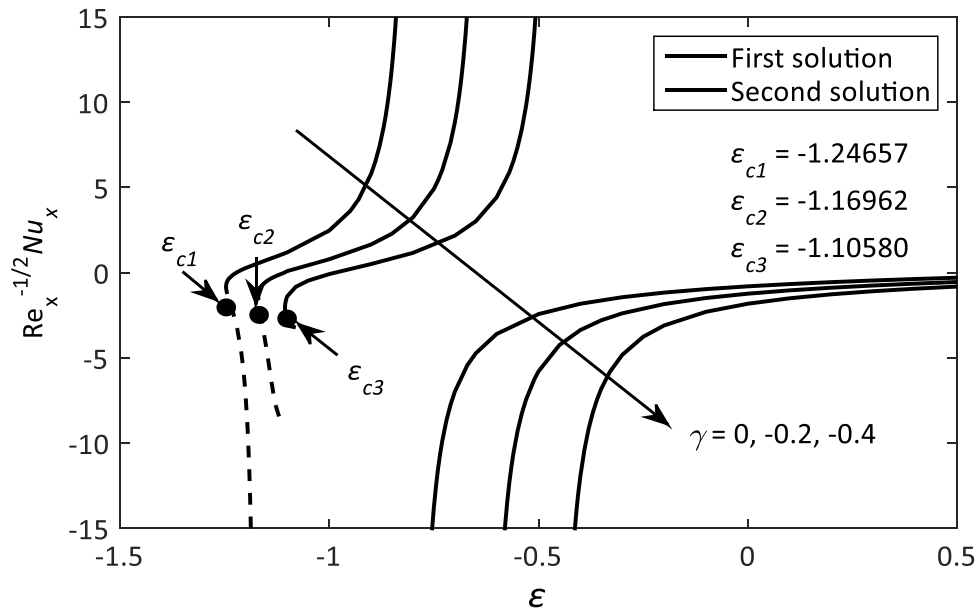


Fig. 3. Variation of the local Nusselt number $Re_x^{-1/2} Nu_x$ with ε for different values of γ when $Pr=1, Q=1$ and $\beta=5$

Figure 4 shows the influence of the heat source parameter Q on the local Nusselt number. It is noticed that the values of $Re_x^{-1/2} Nu_x$, which indicate the heat transfer rate at the surface decrease with an increase in Q .

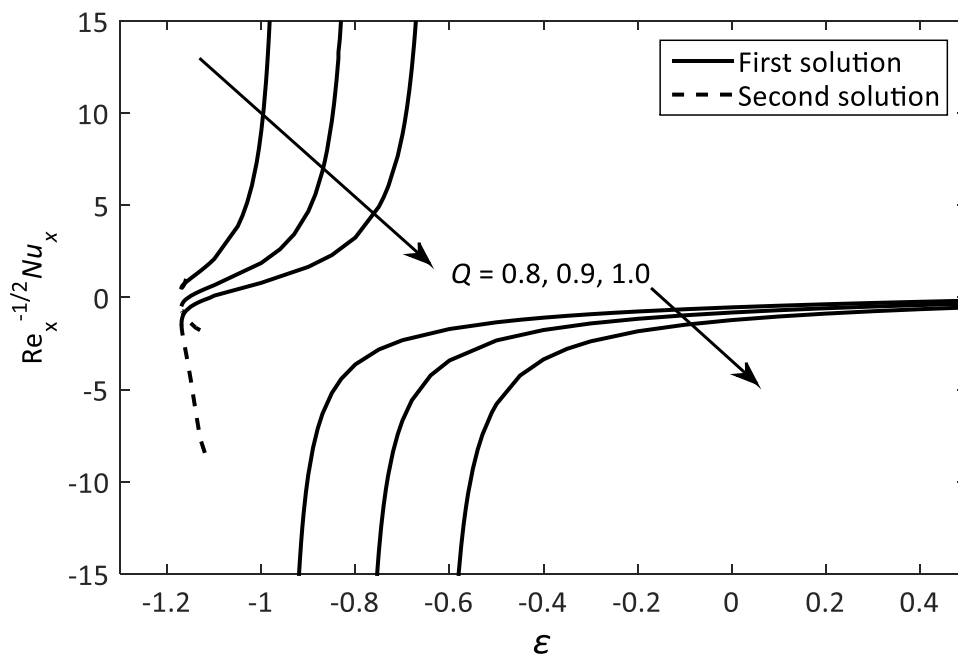


Fig. 4. Variation of the local Nusselt number $Re_x^{-1/2} Nu_x$ with ε for different values of Q when $Pr=1, \gamma=-0.2$ and $\beta=5$

Figures 5 and 6 show the effect of the injection parameter γ on the dimensionless velocity and temperature profiles, respectively. It is seen that the boundary layer thickness for the second solution is higher than that of the first solution, as depicted in Figures 5 and 6. Meanwhile, Figures 5 and 6 show that increasing magnitude of γ is to increase the momentum and thermal boundary layer thicknesses for the first solutions and thus decreasing the velocity and temperature gradients, in consequence decreases the skin friction coefficient and the heat transfer rate at the surface which are consistent with the graphs in Figures 2 and 3. In contrast, the second solution shows an opposite trends.

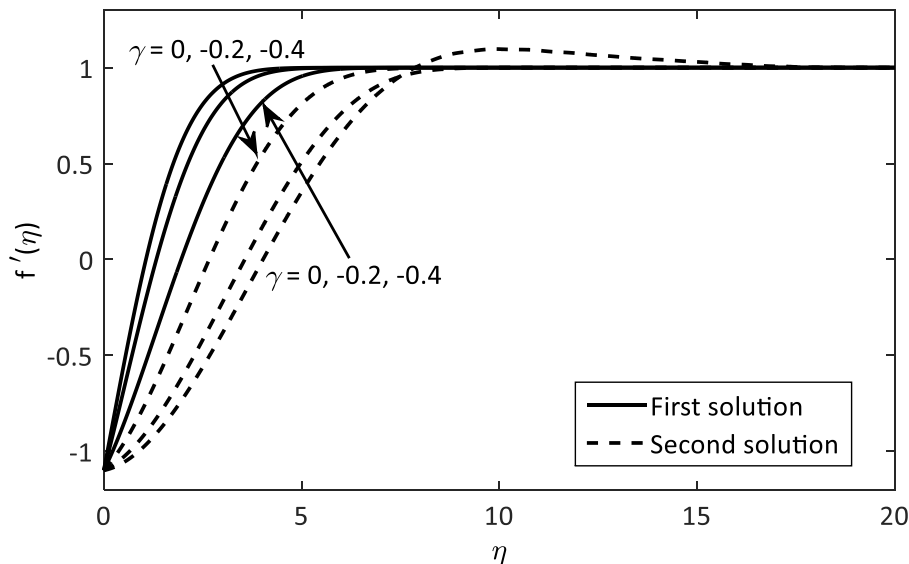


Fig. 5. The velocity profiles $f'(\eta)$ for different values of γ when $Pr = 1$, $Q = 1$, $\beta = 5$ and $\varepsilon = -1.1$ (shrinking case)

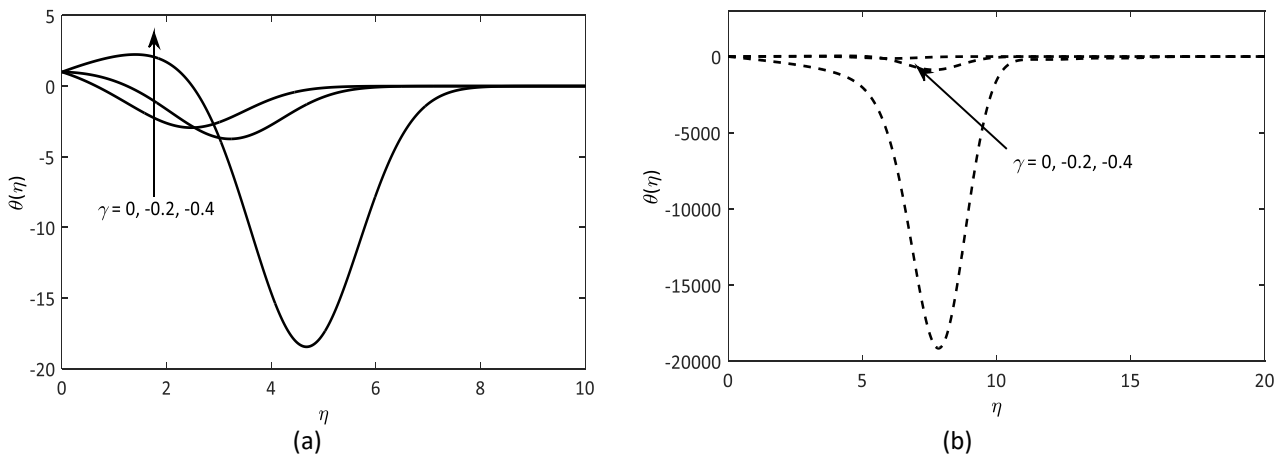


Fig. 6. The temperature profiles $\theta(\eta)$ for (a) first solution and (b) second solution for different values of γ when $Pr = 1$, $Q = 1$, $\beta = 5$ and $\varepsilon = -1.1$ (shrinking case)

It is clear that the temperature decreases as the value of heat source increases as plotted in Figure 7. This is due to the fact that additional energy is generated in the boundary layer in the presence of heat source. This additional energy increases the thickness of the thermal boundary layer, so that decreases the temperature gradient and in consequences the heat transfer rate at the surface is enhanced (reduce) which is consistent with the graph in Figure 4.

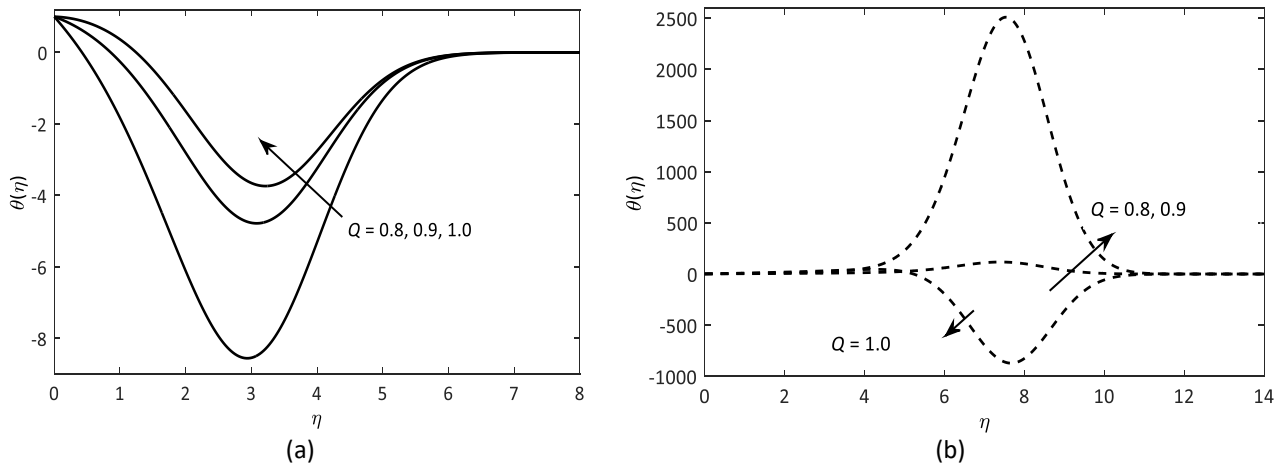


Fig. 7. The temperature profiles $\theta(\eta)$ for (a) first solution and (b) second solution for different values of Q when $Pr=1$, $\gamma=-0.2$, $\beta=5$ and $\varepsilon=-1.1$ (shrinking case)

Furthermore, it is worth highlighting that in all Figures 5-7 presented here, the velocity and temperature profiles satisfy the far field boundary conditions in Eq. (9) asymptotically. This helps to validate the numerical results of the boundary value problem in Eqs. (7)-(9) and the existence of the dual solutions presented in Figures 2-4.

5. Conclusions

In this paper, the problem of the stagnation-point flow and heat transfer over a stretching/shrinking sheet with heat source and injection effect in a Casson fluid was investigated and solved numerically using bvp4c in MATLAB. The analysis shows that the skin friction coefficient and the local Nusselt number as well as the velocity and temperature were influenced by injection parameter, stretching/shrinking parameter and heat source parameter. The skin friction coefficient was not affected by heat source effect. It is also found that the local Nusselt number decreases with an increase in heat source parameter. The skin friction coefficient and the heat transfer rate at the surface decrease as the magnitude of injection parameter increases. Dual solutions were found to exist for the certain range of shrinking strength and the unique solution was exist for the stretching case. The stability analysis has been conducted to show that the first solution is stable, whereas the second solution is unstable.

Acknowledgement

The author would like to acknowledge the support from the Fundamental Research Grant Scheme (FRGS) under a grant number of FRGS/1/2018/STG06/UNIMAP/02/3 from the Ministry of Education Malaysia.

References

- [1] Patel, Manisha, and Munir Timol. "Magneto hydrodynamic orthogonal stagnation point flow of a power-law fluid toward a stretching surface." *Am. J. Comput. Math.* 1 (2011): 129-133.
<https://doi.org/10.4236/ajcm.2011.12013>
- [2] Makinde, O.D., W.A. Khan, and Z.H. Khan. "Buoyancy effects on MHD stagnation point flow and heat transfer of a nanofluid past a convectively heated stretching / shrinking sheet." *Int. J. Heat Mass Transf.* 62 (2013): 526-533.
<https://doi.org/10.1016/j.ijheatmasstransfer.2013.03.049>
- [3] Nandy, S.K., and I. Pop. "Effects of magnetic field and thermal radiation on stagnation flow and heat transfer of nano fluid over a shrinking surface." *Int. Commun. Heat Mass Transf.* 53 (2014): 50-55.

- <https://doi.org/10.1016/j.icheatmasstransfer.2014.02.010>
- [4] Fauzi, N.F., S. Ahmad, and I. Pop. "Stagnation point flow and heat transfer over a nonlinear shrinking sheet with slip effects." *Alexandria Eng. J.* 54, no. 4 (2015): 929-934.
<https://doi.org/10.1016/j.aej.2015.08.004>
- [5] Ramesh, G.K., B.J. Gireesha, T. Hayat, and A. Alsaedi. "Stagnation point flow of Maxwell fluid towards a permeable surface in the presence of nanoparticles." *Alexandria Eng. J.* 55, no. 2 (2016): 857-865.
<https://doi.org/10.1016/j.aej.2016.02.007>
- [6] Mahapatra, T.R., and A.S. Gupta. "Heat transfer in stagnation-point flow towards a stretching sheet." *Heat Mass Transf.* 38, no. 6 (2002): 517-521.
<https://doi.org/10.1016/j.aej.2016.02.007>
- [7] Nazar, Roslinda, Norsarahaida Amin, Diana Filip, and Ioan Pop. "Unsteady boundary layer flow in the region of the stagnation point on a stretching sheet." *Int. J. Eng. Sci.* 42, no. 11–12 (2004): 1241-1253.
<https://doi.org/10.1016/j.ijengsci.2003.12.002>
- [8] Othman, Noor Adila, Nor Azizah Yacob, Norrifah Bachok, Anuar Ishak, and Ioan Pop. "Mixed convection boundary-layer stagnation point flow past a vertical stretching/shrinking surface in a nanofluid." *Appl. Therm. Eng.* 115 (2017): 1412-1417.
<https://doi.org/10.1016/j.applthermaleng.2016.10.159>
- [9] Rehman, Fiaz Ur, S. Nadeem, and Rizwan Ul Haq. "Heat transfer analysis for three-dimensional stagnation-point flow over an exponentially stretching surface." *Chinese J. Phys.* 55, no. 4 (2017): 1552-1560.
<https://doi.org/10.1016/j.cjph.2017.05.006>
- [10] Naganthran, Kohilavani, Roslinda Nazar, and Ioan Pop. "Stability analysis of impinging oblique stagnation-point flow over a permeable shrinking surface in a viscoelastic fluid." *Int. J. Mech. Sci.* 131–132 (2017): 663-671.
<https://doi.org/10.1016/j.ijmecsci.2017.07.029>
- [11] Sharma, P.R., Sharad Sinha, R.S. Yadav, and Anatoly N. Filippov. "MHD mixed convective stagnation point flow along a vertical stretching sheet with heat source/sink." *Int. J. Heat Mass Transf.* 117 (2018): 780-786.
<https://doi.org/10.1016/j.ijheatmasstransfer.2017.10.026>
- [12] Roşca, Alin V., and Ioan Pop. "Flow and heat transfer over a vertical permeable stretching / shrinking sheet with a second order slip." *Int. J. Heat Mass Transf.* 60 (2013): 355-364.
<https://doi.org/10.1016/j.ijheatmasstransfer.2012.12.028>
- [13] Yasin, Mohd Hafizi Mat, Anuar Ishak, and Ioan Pop. "MHD heat and mass transfer flow over a permeable stretching/shrinking sheet with radiation effect." *J. Magn. Magn. Mater.* 407 (2016): 235-240.
<https://doi.org/10.1016/j.jmmm.2016.01.087>
- [14] Naganthran, Kohilavani, Roslinda Nazar, and Ioan Pop. "Unsteady stagnation-point flow and heat transfer of a special third grade fluid past a permeable stretching/shrinking sheet." *Scientific Reports* 6 (2016): Article no. 24632
<https://doi.org/10.1038/srep24632>
- [15] Alam, M.S., M. Asiya Khatun, M.M. Rahman, and K. Vajravelu. "Effects of variable fluid properties and thermophoresis on unsteady forced convective boundary layer flow along a permeable stretching/shrinking wedge with variable Prandtl and Schmidt numbers." *Int. J. Mech. Sci.* 105 (2016): 191-205.
<https://doi.org/10.1016/j.ijmecsci.2015.11.018>
- [16] Jamaludin, Anuar, Roslinda Nazar, and Ioan Pop. "Three-dimensional mixed convection stagnation-point flow over a permeable vertical stretching/shrinking surface with a velocity slip." *Chinese J. Phys.* 55, no. 5 (2017): 1865-1882.
<https://doi.org/10.1016/j.cjph.2017.08.006>
- [17] Jusoh, Rahimah, Roslinda Nazar, and Ioan Pop. "Flow and heat transfer of magnetohydrodynamic three-dimensional Maxwell nanofluid over a permeable stretching/shrinking surface with convective boundary conditions." *Int. J. Mech. Sci.* 124–125 (2017): 166-173.
<https://doi.org/10.1016/j.ijmecsci.2017.02.022>
- [18] Nasir, Nor Ain Azeany Mohd, Anuar Ishak, and Ioan Pop. "Stagnation-point flow and heat transfer past a permeable quadratically stretching/shrinking sheet." *Chinese J. Phys.* 55, no. 5 (2017): 2081-2091.
<https://doi.org/10.1016/j.cjph.2017.08.023>
- [19] Setha, G.S., A.K. Singha, M.S. Mandal, Astick Banerjee., and Krishnendu Bhattacharyya. "MHD stagnation-point flow and heat transfer past a non-isothermal shrinking/stretching sheet in porous medium with heat sink or source effect." *Int. J. Mech. Sci.* 134 (2017): 98-111.
<https://doi.org/10.1016/j.ijmecsci.2017.09.049>
- [20] Hamid, Rohana Abdul, Roslinda Nazar, and Ioan Pop. "Boundary layer flow of a dusty fluid over a permeable shrinking surface." *Int. J. Numerical Methods for Heat Fluid Flow* 27, no. 4 (2017): 758-772.
<https://doi.org/10.1108/HFF-01-2016-0030>

- [21] Soid, Siti Khuzaimah, Anuar Ishak, and Ioan Pop. "MHD flow and heat transfer over a radially stretching/shrinking disk." *Chinese J. Phys.* 56, no. 1 (2018): 58–66.
<https://doi.org/10.1016/j.cjph.2017.11.022>
- [22] Dero, Sumera, Azizah Mohd Rohni, and Azizan Saaban. "MHD micropolar nanofluid flow over an exponentially stretching/shrinking surface: Triple Solutions." *Journal of Advanced Research in Fluid Mechanics and Thermal Sciences* 56, no. 2 (2019) 165-174.
- [23] Yashkun, Ubaidullah, Khairy Zaimi, Nor Ashikin Abu Bakar, and Mohammad Ferdows. "Nanofluid stagnation-point flow using Tiwari and Das model over a stretching/shrinking sheet with suction and slip effects." *Journal of Advanced Research in Fluid Mechanics and Thermal Sciences* 70, no. 1 (2020): 62-76.
<https://doi.org/10.37934/arfmts.70.1.6276>
- [24] Dash, R.K., K.N. Mehta, and G. Jayaraman. "Casson fluid flow in a pipe filled with a homogeneous porous medium." *Int. J. Engng. Sci.* 34, no. 10 (1996): 1145–1156.
[https://doi.org/10.1016/0020-7225\(96\)00012-2](https://doi.org/10.1016/0020-7225(96)00012-2)
- [25] Animasaun, I.L., E.A. Adebile, and A.I. Fagbade. "Casson fluid flow with variable thermo-physical property along exponentially stretching sheet with suction and exponentially decaying internal heat generation using the homotopy analysis method." *J. Niger. Math. Soc.* 35, no. 1 (2016): 1-17.
<https://doi.org/10.1016/j.jnms.2015.02.001>
- [26] Hayat, T., S.A. Shehzad, A. Alsaedi, and M.S. Alhothuali. "Mixed convection stagnation point flow of Casson fluid with convective boundary conditions." *Chinese Phys. Lett.* 29, no. 11 (2012): 114704.
<http://iopscience.iop.org/0256-307X/29/11/114704>
- [27] Bhattacharyya, Krishendu. "Boundary layer stagnation-point flow of Casson fluid and heat transfer towards a shrinking/stretching sheet." *Front. Heat Mass Transf.* 4, 023003 (2013).
<http://dx.doi.org/10.5098/hmt.v4.2.3003>
- [28] Kameswaran, Peri K., S. Shaw, and P. Sibanda. "Dual solutions of Casson fluid flow over a stretching or shrinking sheet." *Sadhana* 39, no. 6 (2014): 1573-1583.
<https://doi.org/10.1007/s12046-014-0289-7>
- [29] El-Aziz, Mohamed Abd, and Aishah S. Yahya. "Perturbation analysis of unsteady boundary layer slip flow and heat transfer of Casson fluid past a vertical permeable plate with Hall current." *Appl. Math. Comput.* 307 (2017): 146-164.
<https://doi.org/10.1016/j.amc.2017.02.034>
- [30] Abdul Hakeem, A. K., P. Renuka, N., Vishnu Ganesh, R. Kalaivanan, and B. Ganga. "Influence of inclined Lorentz forces on boundary layer flow of Casson fluid over an impermeable stretching sheet with heat transfer." *J. Magn. Magn. Mater.* 401 (2016): 354–361.
<https://doi.org/10.1016/j.jmmm.2015.10.026>
- [31] Khan, Muhammad Ijaz, Muhammad Waqas, Tasawar Hayat, and Ahmed Alsaedi. "A comparative study of Casson fluid with homogeneous-heterogeneous reactions." *J. Colloid Interface Sci.* 498 (2017): 85–90.
<https://doi.org/10.1016/j.jcis.2017.03.024>
- [32] Maity, S., S.K. Singh, and A.V. Kumar. "Unsteady three dimensional flow of Casson liquid film over a porous stretching sheet in the presence of uniform transverse magnetic field and suction/injection." *J. Magn. Magn. Mater.* 419 (2016): 292–300.
<https://doi.org/10.1016/j.jmmm.2016.06.004>
- [33] Medikare, Monica, Sucharitha Joga, and Kishore Kumar Chidem. "MHD stagnation point flow of a Casson fluid over a nonlinearly stretching sheet with viscous dissipation." *Am. J. Comput. Math.* 6, no. 1 (2016): 37–48.
<https://doi.org/10.4236/ajcm.2016.61005>
- [34] Raju, C.S.K., and N. Sandeep. "Unsteady Casson nanofluid flow over a rotating cone in a rotating frame filled with ferrous nanoparticles : A numerical study." *J. Magn. Magn. Mater.* 421 (2017): 216-224.
<https://doi.org/10.1016/j.jmmm.2016.08.013>
- [35] Raju, C.S.K. and N. Sandeep. "MHD slip flow of a dissipative Casson fluid over a moving geometry with heat source/sink: A numerical study." *Acta Astronautica* 133 (2017): 436–443.
<https://doi.org/10.1016/j.actaastro.2016.11.004>
- [36] Raju, C.S.K., Mohammad Mainul Hoque, and T. Sivasankar. "Radiative flow of Casson fluid over a moving wedge filled with gyrotactic microorganisms." *Adv. Powder Technol.* 28, no. 2 (2017): 575–583.
<https://doi.org/10.1016/j.appt.2016.10.026>
- [37] Rehman, Khalil Ur, Aqeela Qaiser, M.Y. Malik, and U. Ali. "Numerical communication for MHD thermally stratified dual convection flow of Casson fluid yields by stretching cylinder." *Chinese J. Phys.* 55, no. 4 (2017): 1605–1614.
<https://doi.org/10.1016/j.cjph.2017.05.002>

-
- [38] Shateyi, S., F. Mabood, and G. Lorenzini. "Casson fluid flow: Free convective heat and mass transfer over an unsteady permeable stretching surface considering viscous dissipation." *J. Eng. Thermophys.* 26, no. 1 (2017): 39-52.
<https://doi.org/10.1134/S1810232817010052>
- [39] Alkawasbeh, Hamzeh Taha. "Numerical solution of micropolar Casson fluid behaviour on steady MHD natural convective flow about a solid sphere." *Journal of Advanced Research in Fluid Mechanics and Thermal Sciences* 50, no. 1 (2018): 55-66.
- [40] Bhattacharyya, Krishnendu. "MHD stagnation-point flow of Casson fluid and heat transfer over a stretching sheet with thermal radiation." *J. Thermodyn.* 2013, 169674 (2013).
<https://doi.org/10.1155/2013/169674>
- [41] Weidman, P.D., D.G. Kubitschek, and A.M.J. Davis. "The effect of transpiration on self- similar boundary layer flow over moving surfaces." *Int. J. Eng. Sci.* 44, no. 11-12 (2006): 730–737.
<https://doi.org/10.1016/j.ijengsci.2006.04.005>